^{31}P and ^{1}H MRS of human cancer

V. L. Doyle*, S. J. Barton and J. R. Griffiths

CRC Biomedical Magnetic Resonance Research Group, Department of Cellular and Molecular Sciences, Division of Biochemistry, St George's Hospital Medical School, Cranmer Terrace, London, SW17 0RE, UK

Magnetic resonance spectroscopy (MRS) provides a powerful tool in the study of human cancer. Biochemical information obtained by MRS indicates how the metabolism of tumours differs from that of normal tissue; it provides diagnostic information on tumour type and grading, and may be used to monitor the efficacy of anticancer treatments. ^{31}P and ^{1}H are the most widely used nuclei in clinical MRS studies of cancer, giving complementary biochemical information, though MRS studies of drug metabolism using ^{19}F are also under investigation. This paper describes recent research using ^{31}P and ^{1}H MRS in the study of human cancers *in vivo*.

^{31}P MRS of human cancer

^{31}P MRS provides a valuable method of monitoring the cellular energy balance and metabolism of tumours for cancer research. It also provides a non-invasive method of monitoring response to treatment and selecting appropriate therapy. Typical *in vivo* ^{31}P spectra have three peaks due to nucleotide triphosphates (predominantly ATP, the major source of cellular energy); a peak due to phosphocreatine (PCr, a short term energy reserve); and an inorganic phosphate (Pi) peak, a product of the breakdown of ATP to ADP (adenosine diphosphate). The intracellular pH may be determined by measuring the chemical shift of the Pi peak with respect to a reference peak (usually that of PCr, although the ATP peaks can be used if PCr is absent).

^{31}P MRS of tumours

The Pi peak is often pronounced in tumours, but (contrary to expectations) their intracellular pH is usually close to neutral. There may also be visible peaks due to PME (phosphomonoester compounds) including phosphocholine, phosphoethanolamine, glucose-6-phosphate, glycerol-3-phosphate and AMP (adenosine monophosphate), and to PDE (phosphodiester compounds) including GPE (glycerophosphoethanolamine) and GPC (glycerophosphocholine). ^{31}P MR tumour spectra exhibit elevated PME signals (from phospholipid (PL) precursors) and PDE signals (from phospholipid (PL) catabolites) compared to normal tissue spectra. The peaks of these signals vary greatly in different tumours and change significantly during tumour growth and response to therapy. There have been many reports of changes in the ^{31}P spectra of tumours as a result of successful therapy[1]. For instance, increased PDE/PME was reported in sarcoma[2]; increased PME/ATP[3] and increased PDE/β-ATP[4] in non-Hodgkin's lymphoma, and increased Pi/PME in lymphoma[5]. These suggestive results have prompted a multi-centre trial funded by the National Cancer Institute (USA) to see whether the fall in the PME peak during successful chemotherapy can be used as a predictor of tumour response.

^{31}P MRS in breast cancer

A preliminary study from this trial used 3D chemical shift imaging (CSI)[6,7] to acquire ^{31}P spectroscopic data sets from patients with primary breast cancer. When interpreting data from breast studies it is important to be aware of the fact that the ^{31}P spectrum acquired from the breast is dependent upon the age, menopausal status, stage of the menstrual cycle[8] and whether the breast is lactating or not[9]. Due to these profound morphological and physiological changes that occur in the breasts of healthy women it is difficult to define the 'normal' ^{31}P spectrum against which a tumour spectrum can be compared and the degree of malignancy determined. For this reason 3D CSI was the chosen method of spectroscopic localization since spectra may be acquired from both the tumour and adjacent tissue in the same data set. This may allow spectra from tumour and 'normal' breast tissue in the same patient to be compared, and heterogeneity in larger tumours can be demonstrated. Such comparisons may aid the interpretation of spectral changes in response to therapy.

Figure 1 shows the central slice from a 3D CSI data set acquired from a 51-year-old patient with an infiltrative ductal carcinoma. The data were acquired on a 1.5 T SIGNA (GE, Milwaukee). Regions of normal chest wall muscle and breast tumour (Figure 1 *b* and *c*) can be clearly differentiated. The tumour spectrum demonstrates high PME and Pi signals relative to the NTPs. Variability of PME across the breast is observed. Figure 1 *d* is a spectrum acquired from a region containing both

*For correspondence. (email: vdoyle@sghms.ac.uk)

Table 1. Mean metabolite levels expressed as a percentage of the total ^{31}P signal for 3 patients and a normal volunteer

	PME	Pi	PDE	PCr	NTP	PME/NTP	pH
Breast tumour 1 (51 years)	27%	11%	25%	6%	10%	2.7	NQ*
Breast tumour 2 (59 years)	23%	10%	29%	2%	12%	1.9	7.8[a†]
Breast tumour 3 (43 years)	23%	16%	32%	–	10%	2.3	7.5[a]
Normal breast (52 years)	17%	8%	34%	–	14%	1.2	7.2[a]
Chest muscle (52 years)	–	5%	6%	51%	13%	NQ	7.1[b]

NTP is the average of the three NTP peaks. Normal breast and chest wall muscle values are from the normal volunteer. NQ = not quantifiable. *The pH for the first breast tumour was alkaline but outside the range of our calculations. †This value was at the limits of our calculation due to the poor S/N. It is unlikely that a tumour would have a pH as low as 7.8. [a]pH from the Pi-αNTP chemical shift difference, [b]pH from the Pi–PCr chemical shift difference.

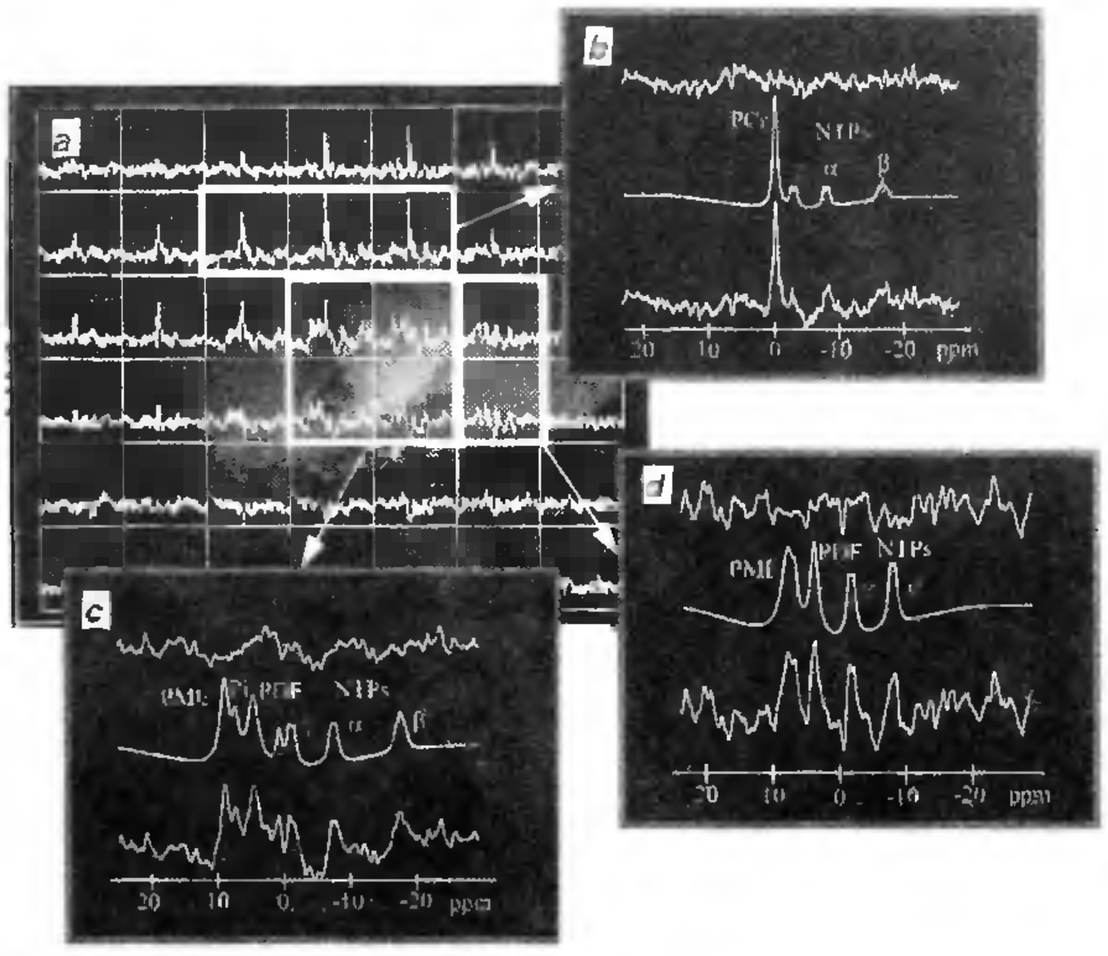

Figure 1. *a*, Phased ^{31}P spectra from the breast of a 51-year-old patient with an infiltrative ductal carcinoma; *b*, Muscle spectrum (bottom), VARPRO fit (middle) and residual (top), *c*, Breast tumour spectrum (bottom), VARPRO fit (middle) and residual (top). Note the elevated PME and PDE compared to normal breast; *d*, Spectrum from a mixture of normal breast and breast tumour (bottom), VARPRO fit (middle) and residual (top).

normal breast tissue and breast tumour. The level of PME which was markedly elevated in the tumour spectrum is now comparable to the NTP signal. The PCr is mostly localized to the chest wall and the small peak at 0 ppm in the tumour spectrum most likely arises from contaminating muscle signal. Table 1 summarizes the results of an initial study of 3 patients with breast cancer (pre-treatment) and a normal volunteer, demonstrating the elevated PME and PDE in breast tumour compared to normal breast tissue. These data agree with previous MRS studies in which non-localized spectra were acquired from breast tumours[10] and normal breast tissues[9]. They also demonstrate elevated PME but no PCr in breast tumours compared with adjacent chest wall muscle and a more alkaline pH. High levels of PME in tumours are thought to be related to rapid cell proliferation and/or cell death[1,11]. PCr in the first two breast tumour spectra is probably due to Fourier bleed from adjacent chest wall muscle.

Monitoring response to treatment using ^{31}P MRS

A further study is presently underway to monitor the response to treatment in non-Hodgkin's lymphoma (NHL) patients undergoing chemotherapy using the same data acquisition techniques as in the previous study. This study will investigate the use of the ^{31}P 3D CSI method to identify responding tumours prior to any volume or imaging changes. This will enable ineffective therapy to be stopped and an appropriate therapy regime to be initiated, preventing extended, unnecessary patient anxiety and providing a more optimistic outlook for therapeutic response. In these studies, proton decoupling techniques have also been employed to improve spectral resolution and signal-to-noise[12]. Figure 2 shows pre- and post-treatment data from a 77-year-old male patient with an NHL in his groin. It can be seen that there are large PME peaks in both scans, indicative of the disease. Table 2 shows the ^{31}P metabolite peak areas before and after the treatment. The PME/PDE ratios are reduced post-treatment, indicating response. At the time of the second scan there was no observable change in tumour volume using palpation or MRI. This is one example of the application of ^{31}P MRS as a non-invasive tool in monitoring response of tumours to treatment.

^{1}H MRS of human cancer

^{1}H MRS is technically difficult in most parts of the body; however, it is widely used to study the brain (and also prostate), and particularly intracranial tumours. The nature of the metabolites detected in single voxel ^{1}H MR spectra depends on the echo time. At long echo-times (240–270 ms), *N*-acetyl aspartate (NAA), total creatines (tCr), total cholines (tCho), alanine, and lactate are observed. At 136 ms an out-of-phase, inverted lactate and alanine peak may be observed, while at short echo times

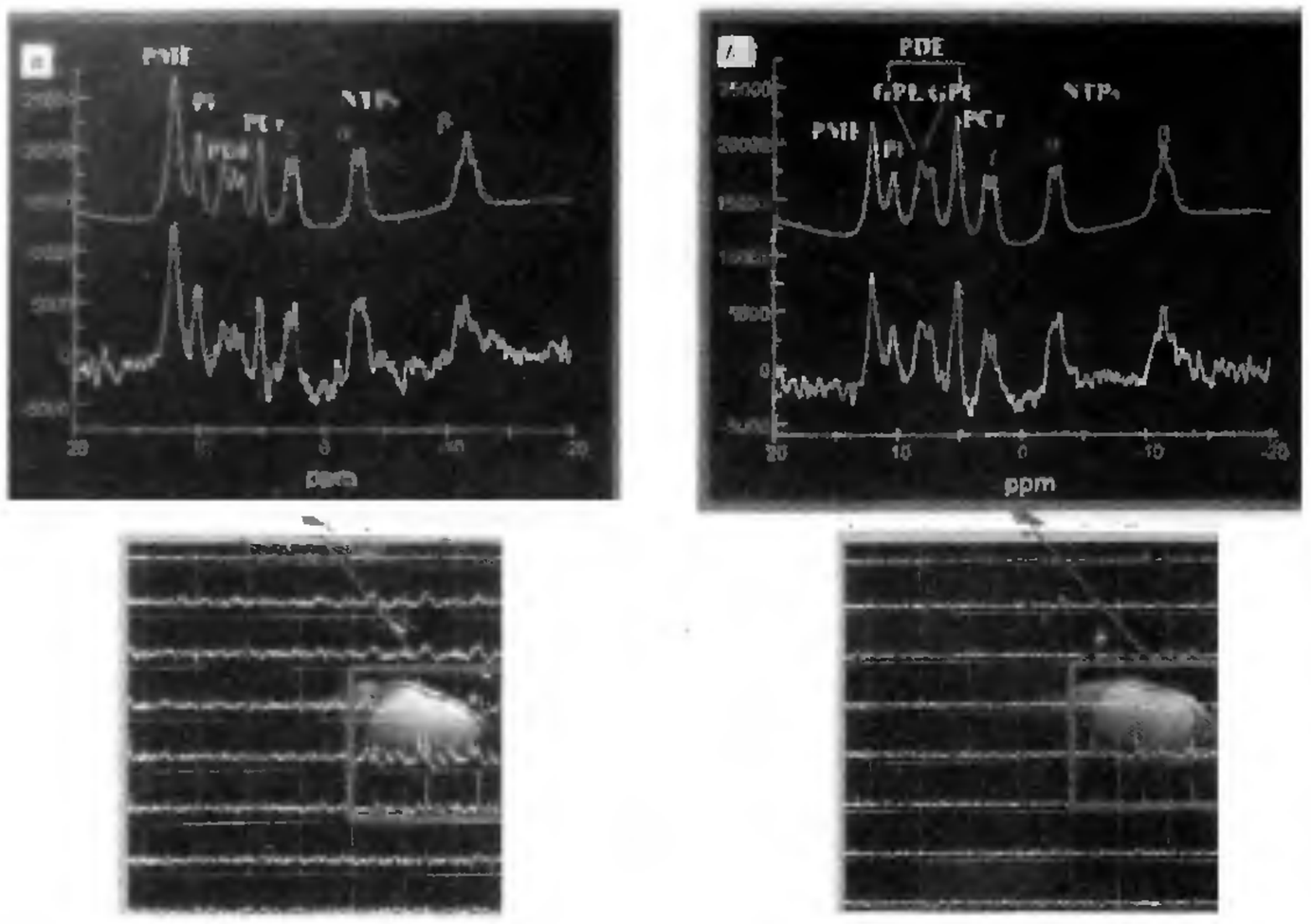

Figure 2. Phased ^{31}P spectra from a 77-year-old male patient with a NHL in his groin. *a*, Pre-treatment spectrum showing NHL spectrum (bottom) and the VARPRO fit (top), *b*, Post-treatment spectrum showing NHL spectrum (bottom) and the VARPRO fit (top).

Table 2. Metabolite ratios pre- and post-treatment for a 77-year-old male patient with an NHL in his groin

	PME/NTP	Pi/NTP	PDE/NTP	PME/PDE
Pre-treatment	2.0	0.8	0.3	1.5
Post-treatment	1.2	0.7	1.7	0.7

(20–50 ms) *myo*-inositol, glutamate/glutamine and lipids may also be present.

^{1}H MRS of brain tumours – Determining type and grade

Several studies have shown that ^{1}H NMR spectra of human brain tumours differ significantly from those of healthy brain tissues[1]. Tumour cells which are non-neuronal in origin (most primary brain tumours and all metastases), lack NAA but may contain other *N*-acetyl compounds. When present in a spectrum, NAA is most likely to come from the normal brain tissue within an infiltrative tumour, so the signal will be greatly reduced compared to the normal brain tissue[13]. The resonance labelled tCho is derived from free choline, phosphocholine and glycerophosphocholine. The signal is elevated in low grade tumours compared to the normal brain[14] and has been attributed to increased cell membrane synthesis in rapidly proliferating tissue and an increase in the visibility of choline due to cell membrane damage. In aggressive, high-grade tumours the tCho concentration is reduced, perhaps due to areas of necrosis which dilute the choline concentration in the tumour tissue. Creatine, a marker for brain cell density, is generally reduced in tumours compared to normal white matter. Alanine is considered to be a specific marker in meningioma spectra[15], and lactate (the end-product of anaerobic respiration) has been observed in metastases[16] and glial brain tumours[15]. Glutamate and glutamine are also observed as a combined peak in meningiomas and low grade astrocytomas. Lipid signals are often present in brain tumour spectra and arise from the presence of mobile lipid molecules rather than lipid-bilayers in membranes. The amount of lipid has been correlated with the extent of necrosis[17] and malignancy[18]. If present, the lipid peak may obscure alanine or lactate. To resolve these resonances, metabolite-nulling techniques[19] have been used, in which lipid and macromolecule signals are edited from the spectrum[20]. Figure 3 shows images and single-voxel spectra of high and low grade gliomas.

There is currently much interest in employing ^{1}H MRS in diagnosis and grading of brain tumours, as the metabolite profile differs between tumours of different types and grades. The heterogeneous nature of tumours means that single-voxel spectroscopy has inherent limitations here, though this is also true of tumour biopsy, the current method of diagnosis: neither are representative of the whole tumour. CSI methods in which spectra from multiple voxels are acquired over a large area, are probably more appropriate for diagnosis. A successful approach has been to use pattern recognition techniques to make statistical comparisons of the intensities of all peaks in the spectrum. Grading of gliomas and differentiation from other tumour types and grades has been achieved using this approach[21]. Methods of classification based on single voxel techniques have also shown

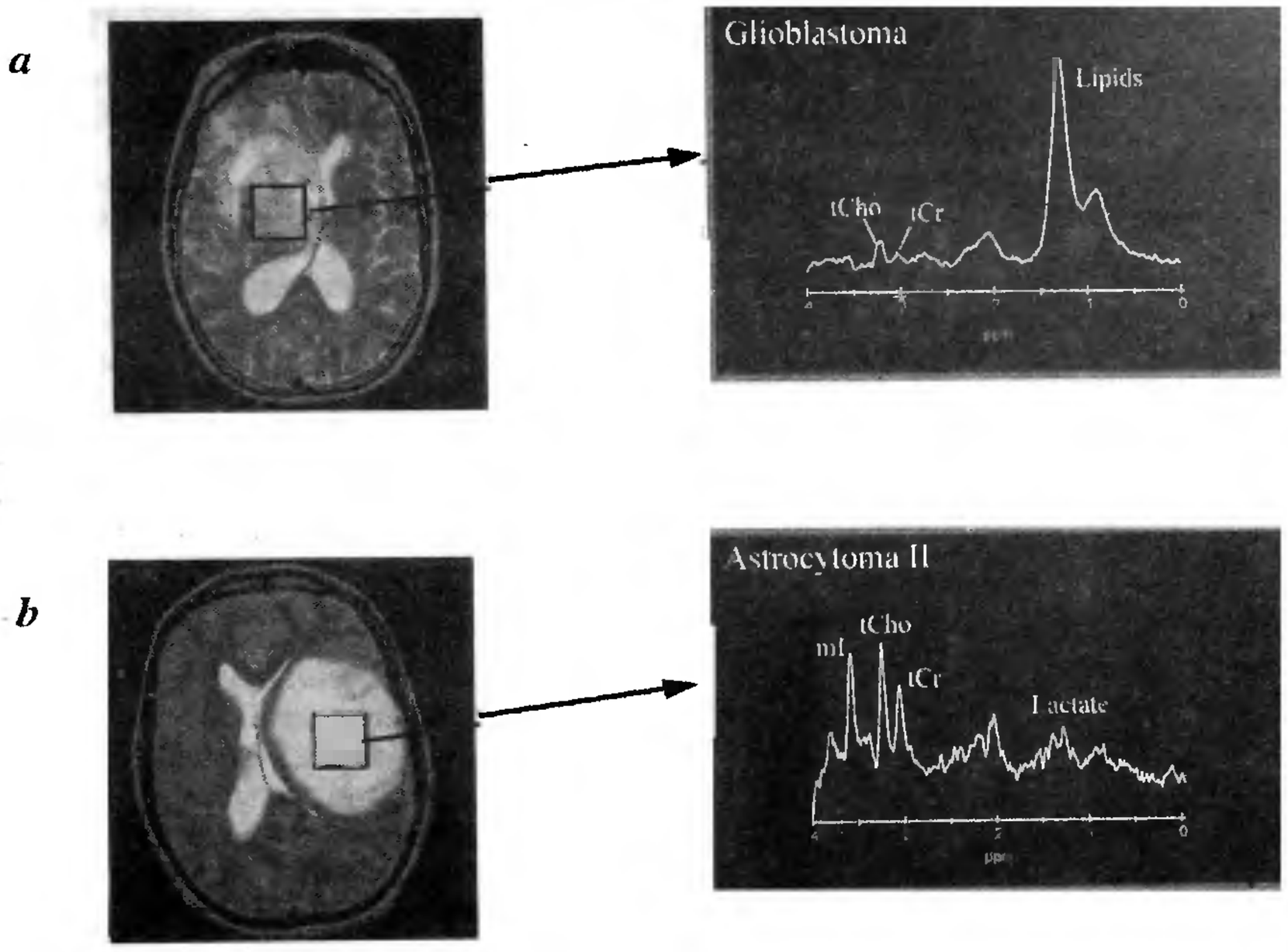

Figure 3. Images of (*a*), high and (*b*), low grade gliomas with the corresponding ^{1}H spectra from the defined region chosen for a single voxel study.

promise in attempts to classify the four most common types of brain tumour: meningiomas, astrocytic tumours, oligodendrogliomas and metastases[22]. Since adult human brain tumours do not respond well to chemotherapy, there is currently limited scope for MRS to monitor response, although it has been used to monitor response to radiotherapy and to differentiate radiation fibrosis from possible tumour recurrence[23].

Discussion

This paper has demonstrated the wealth of information that may be obtained non-invasively using ^{31}P and ^{1}H MRS in the study of human cancer *in vivo*. ^{31}P MRS may be used to monitor response to therapy and to prevent ineffective therapy from being continued and allow replacement by a more appropriate therapy regime. ^{1}H MRS enables the type and grade of brain tumours to be determined without the need for surgical biopsy. This may help to reduce patient mortality when the tumour is in a technically difficult position to reach surgically. In addition, unnecessary operations to remove non-malignant tumours may be avoided.

MRS has remained tantalizingly close to practical application for several years, though to date it is still primarily a research tool. Hopefully, with more public awareness and the rapid development of this technique over the next couple of years we will soon see the application of MRS in the clinical situation.

1. Negendank, W., *NMR Biomed.*, 1992, **5**, 303–324.
2. Koutcher, J. A., Ballon, D., Graham, M., Healey, J. H., Casper, E. S., Heelan, R. and Gerweck, L. E., *Magn. Reson. Med.*, 1990, **16**, 19–34.
3. Bryant, D. J., Bydder, G. M., Case, H. A., Collins, A. G., Cox, I. J., Makepeace, A. and Pennock, J. M., *J. Comput. Assist. Tomogr.*, 1988, **12**, 770–774.
4. Smith, S. R., Martin, P. A., Davies, J. M., Edwards, R. H. T. and Stevens, A. N., *Br. J. Cancer*, 1990, **61**, 485-490.
5. Redmond, O. M., Stack, J. P., O'Connor, N. G., Codd, M. B. and Ennis, J. T., *Br. J. Radiol.*, 1991, **64**, 210–216.
6. Brown, T. R., Kincaid, B. M. and Ugurbil, K., *Proc. Natl. Acad. Sci. USA*, 1982, **79**, 3523–3526.
7. Maudsley, A. A., Hilal, S. K., Perman, W. H. and Simon, H. E., *J. Magn. Reson.*, 1983, **51**, 147–152.
8. Payne, G. S., Dowsett, M. and Leach, M. O., *The Breast*, 1994, **3**, 20–23.
9. Twelves, C. J., Lowry, M., Porter, D. A., Dobbs, N. A., Graves, P. E., Smith, M. A. and Richards, M. A., *Br. J. Radiol.*, 1994, **67**, 36–45.
10. Lowry, M., Porter, D. A., Twelves, C. J., Heasley, P. E., Smith, M. A. and Richards, M. A., *NMR Biomed.*, 1992, **5**, 37–42.
11. Kalra, R., Wade, K. E., Hands, L., Styles, P., Camplejohn, R., Greenall, M., Adams, G. E., Harris, A. L. and Radda, G. K., *Br. J. Cancer*, 1993, **67**, 1145–1153.
12. Li, C.-W., Kuesel, A. C., Padavic-Shaller, K. A., Murphy-Boesch, J., Eisenberg, B. L., Schmidt, R. G., von Roemeling, R. W., Patchefsky, A. S., Brown, T. R. and Negendank, W. G., *J. Cancer Res.*, 1996, **56**, 2964–2973.

13. Frahm, J., Bruhn, H., Hänicke, W., Merboldt, K.-D., Mursh, K. and Markakis, E., *J. Comput. Assist. Tomogr.*, 1991, **15**, 915–22.
14. Gill, S., Thomas, G., van Bruggen, N., Gadian, D., Peden, C., Bell, J., Cox, I., Menon, D., Iles, R., Bryant, D. and Coutts, G., *J. Comput. Assist. Tomogr.*, 1990, **14**, 497–504.
15. Bruhn, H., Frahm, J., Gyngell, M., Merboldt, K.-D., Hänicke, W., Sauter, R. and Hamburger, C., *Radiology*, 1989, **172**, 541–548.
16. Sijens, P., Knopp, M., Brunetti, A., Wicklow, K., Alfano, B., Bachert, P., Saunders, J. A., Stillman, A. E., Kelt, H., Santer, R. and Oudkerk, M., *Magn. Reson. Med.*, 1995, **33**, 818–826.
17. Mountford, C. and Tattersall, M., *Cancer Surv.*, 1987, **6**, 285–314.
18. Kuesal, A., Sutherland, G., Halliday, W. and Smith, I., *NMR Biomed.*, 1994, **7**, 149–155.
19. Behar, K., Rothman, D., Spencer, D. and Petroff, O., *Magn. Reson. Med.*, 1994, **32**, 294–302.
20. Howe, F., McLean, M., Saunders, D., Bell, B. and Griffiths, J., in Proceedings of the SMR 3rd Annual Meeting, Nice, 1995, p. 1705.
21. Pruel, M., Caramanos, Z., Collins, D., Villemure, J.-R., Leblanc, R., Olivier, A., Pokrupa, R. and Arnold, D. L., *Nature Med.*, 1996, **2**, 323–325.
22. Tate, A. R., Griffiths, J. R., Martínez-Pérez, I., Moreno, A., Barba, I., Cabañas, M. E., Watson, D., Alonso, J., Bartumeus, F., Isamat, F., Ferrer, I., Vila, F., Ferrer, E., Capdevila, A. and Arús, C., *NMR Biomed.*, 1998, **11**, 177–191.
23. Cousins, J., Seymour, P., Weaver, S., Emrich, J., Dollar, J., King, V. and Wagle, W., in Proc. ISMRM 5th Annual Meeting, Vancouver, 1997, p. 1141.

ACKNOWLEDGEMENT. The MRS work is supported by the Cancer Research Campaign UK [SP1971/0404] and a grant from the National Cancer Institute [CA62558-04] as part of the 'Co-operative Group on MRS Applications to cancer'.